PHOTOLUMINESCENCE-BASED CURRENT-VOLTAGE CHARACTERISATION OF INDIVIDUAL SUBCELLS IN MULTI-JUNCTION DEVICES

Diego Alonso-Álvarez[*,1], David Lackner[2], Simon P. Philipps[2], Andreas W. Bett[2] and Nicholas Ekins-Daukes[1]
[1]Imperial College London, London, United Kingdom
[2]Fraunhofer Institute for Solar Energy Systems ISE in Freiburg, Germany
[*]Phone: +44 (0) 20 7594 7563, e-mail: d.alonso-alvarez@imperial.ac.uk

ABSTRACT: We demonstrate a photoluminescence based, contactless method to determine the current-voltage characteristics of the individual subcells in a multi-junction solar cell. The method, furthers known results for single junction devices and relies upon the reciprocity relation between the absorption and emission properties on a solar cell. Laser light with a suitable energy is used to excite carriers selectively in one junction and the internal voltages are deduced from the intensity of the resulting luminescence. The IV curves obtained this way on 1J, 2J and 6J devices are compared to those obtained using electroluminescence. Good agreement is obtained at high injection conditions while discrepancies at low injection are attributed to in-plane carrier transport.
Keywords: III-V semiconductors, solar cell, characterization, photoluminescence

1 INTRODUCTION

Rapid and sustained growth of photovoltaic industry requires the development of fast and reliable tools for solar cell characterization. Evaluation of material and device properties is critical for the study of fundamental solar cell physics, determining ways of improving device performance and optimizing the fabrication technologies. This is especially important for III-V multi-junction (MJ) solar cells that need to further reduce fabrication costs and increase efficiencies in order to see a higher penetration in the PV market.

In this work we develop a photoluminescence-based contactless method for current voltage (IV) characterization of MJ solar cells. Laser light is employed for selective carrier photogeneration in component junctions and the free energy of the electron-hole pairs is measured from a photoluminescence (PL) signal. While this technique has been used for characterising single junction devices [1],[2], its extension to MJ devices has been limited, despite the remarkable opportunity it offers. The advantages of the method include:

- independent biasing of component junctions in a multi-junction solar cell for estimation of IV curves of each of the sub-cells;
- no need to account for series resistance;
- compatibility with both completed and partially finished solar cells. The method can be performed at every stage of the device fabrication – for example after the fabrication of each subcell - and used for monitoring and improving the manufacturing steps.

Electroluminescence (EL) has been used for characterising the internal voltages of MJ solar cells with excellent results [3], being the main disadvantage that it can only be applied on completely finished devices and the likely presence of luminescence coupling between subcells. Here we make analogous measurements using PL and compare them with data from EL experiments.

2 THEORETICAL BACKGROUND

The luminescence (photon flux) of a solar cell ϕ_{em} and their external quantum efficiency Q_e are related by the spectral reciprocity relation, given by [3]:

$$\phi_{em}(E) = Q_e(E)\phi_{bb}(E)\left[exp\left(\frac{qV}{kT}\right) - 1\right], \quad [1]$$

with ϕ_{bb} the emission of a black body, V the internal voltage of the cell, equal to the quasi-Fermi level separation, and $V_T=kT/q$ the thermal voltage. Considering that the luminescence is measured in arbitrary units and using the Boltzmann approximation, the internal voltage V_j of a particular junction j in a MJ solar cell can be written as:

$$V_j = V_T \ln\left(\phi_{em}^j\right) + \frac{E}{q} - 2V_T \ln(E) - V_T \ln\left(Q_e^j\right) - C, \quad [2]$$

with C a constant that is determined during the calibration. In EL-based IV, the injected current density J_{inj} is given by the electrically injected current divided by the area of the device – usually defined by an etched mesa. In PL-based IV, J_{inj} is given by:

$$J_{inj} = J_{ex} = \frac{qP_{ex}Q_e(E_{ex})}{E_{ex}A_{ex}} \quad [3]$$

where P_{ex} is the laser power, E_{ex} the energy per photon, and A_{ex} the area of the excitation spot. This equation assumes that all photogenerated carriers contribute to the internal voltage of the cell in the A_{ex} area, $J_{inj} = J_{ex}$. As we will see below, this assumption is incorrect at low injection levels.

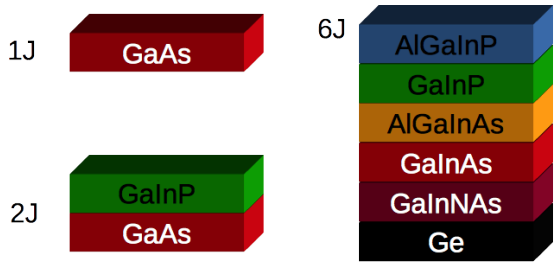

Figure 1: Structure of the solar cells used in this work [4].

3 EXPERIMENT AND MATERIALS

3.1 Solar Cells

We analyse three solar cells with 1, 2 and 6 junctions. The 1J device, made of GaAs was used to calibrate the

setup – find out the value of *C* in Eq. 2. The 2J device is made of GaInP/GaAs whereas the 6J device is a structure involving a dilute nitride 1 eV subcell lattice matched to Ge (see Fig. 1) [4]. The structures were processed in the form of devices with a dense front metal grid suitable for concentration/high injection measurements.

3.2 Experimental setup

EL and PL measurements shared the same collection optics: a doublet of lenses collected the light emitted by the samples and focused it into an optic fibre tip. The relation of the focal lengths of the lenses and the size of the core of the fibre gave a circular collection area of 650 µm in diameter. The fibre was connected to a fast Ocean Optics HR4000 spectrometer for measuring emission between 300 and 1000 nm, or to a grating spectrometer with an un-cooled InGaAs detector at the output for emission between 1000 nm and 1800 nm. A halogen lamp with known spectral shape was used to correct the measurements for the spectral response of the system.

Samples were positioned such that the collection spot was centered in the device. For PL experiments, a continuous wave Nd:YAC laser or a tunable Ti:Sapphire laser were used. The excitation spot was oval, 1200x1450 µm, completely covering the collection region with homogeneous illumination. The geometry and position of the sample was kept constant between measurements, ensuring that the same region is probed in both EL and PL experiments and that the calibration is also common.

QE measurements were taken using a spot size for the monochromatic light also of ~650 nm and probing the same region of the solar cell as for the EL/PL experiments. Since the QE is influenced by the shadowing of the metal grid, it is important to ensure similar measurement areas in order to have a common correction factor *C* for all samples, regardless of the exact metal grid design.

4 EXPERIMENTAL RESULTS

4.1 Calibration

Fig. 2 shows the EL spectra of the 1J GaAs sample as a function of the injected current, from 0.6 mA to 50 mA, and the calculated internal voltage using Eq. 2. This equation requires knowledge of *C* and the procedure to obtain its value is as described in [3]: the voltages are first calculated with C=0 and then they are shifted using a non-zero value for C, such that at a current equal to the short circuit current at 1 Sun, the voltage is equal to the corresponding open circuit voltage. Fig. 2c shows the resulting EL-based IV curve and the comparison with the measured dark IV of the device. As it can be seen, the agreement between both curves is very good at low injection levels. At higher levels, the measured dark IV becomes affected by series resistance while the the EL-based IV, free of series resistance, follows the expected diode shape. The whole curve can be fitted with a 2-diode model, giving saturation current densities of and $J_{01} = 1.5{\times}10^{-17}\ mA/cm^2$ and $J_{02} = 7.8{\times}10^{-8}\ mA/cm^2$ for the $n = 1$ and $n = 2$ components, respectively.

Fig. 2c also shows the IV curve calculated from PL measurements (730 nm excitation, from 1.1 mW to 80 mW) using the same calibration factor that for EL. While the voltages are roughly the same – as expected considering that the EL and PL spectra almost overlap each other in this current and laser power range – currents appear to be overestimated. We will return to this discrepancy below.

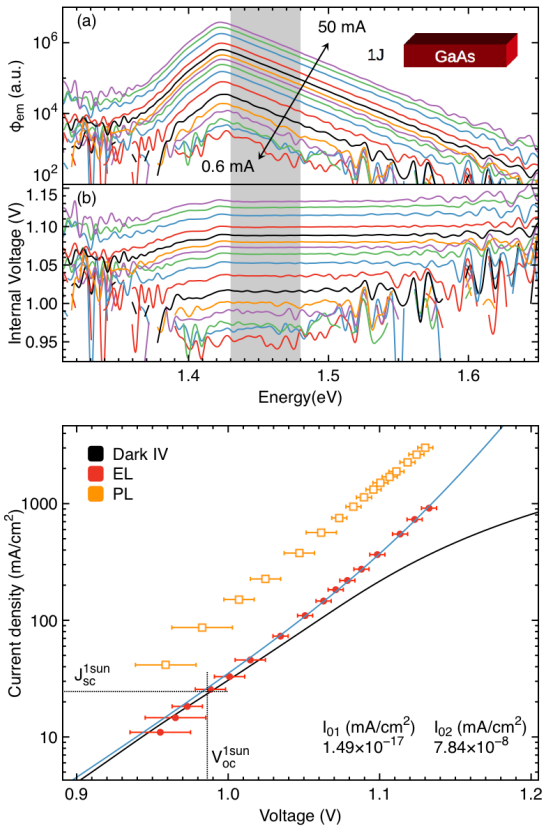

Figure 2: (a) EL emission from the 1J GaAs sample. (b) Calculated internal voltages, including the correction factor, as a function of energy, fairly constant over the high energy side of the EL peak. (c) Implied IV curves from EL and PL measurements and comparison to the normal dark IV curve. The values of J_{01} and J_{02} are the result of fitting the EL-based IV to a 2-diode model.

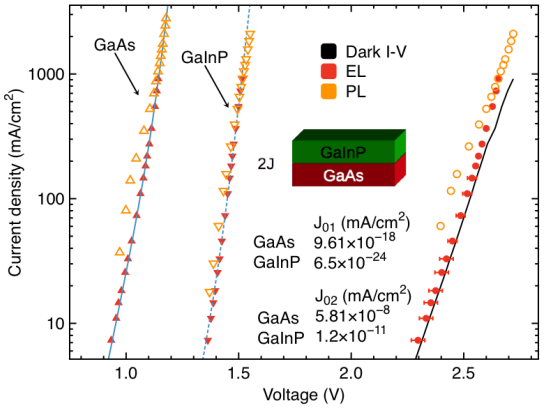

Figure 3: Implied IV curves from EL and PL of the 2J solar cell, as well as the total IV curves and the dark IV. The values of J_{01} and J_{02} are the result of fitting the EL-based IV to a 2-diode model.

4.2 2J GaInP/GaAs solar cell

The same experiments were conducted on the 2J device using a 532 nm laser for the GaInP subcell and a

730 nm laser for the bottom subcell. The power range was the same in both cases, from 1.1 mW to 80 mW. The correction factor *C* remains as obtained previously.

Fig. 3 shows the resulting IV curves for each subcell and the total IV curve calculated by adding together the voltages at a given current. The IV curved derived from EL follows a 2-diode model closely and the total IV is very similar to the dark IV at low injection, diverging just at higher values when the latter is influenced by series resistance. As with the 1J, the PL derived IV results in higher current than derived from EL at low injection, yet converging at higher injection. For the case of GaInP, this effect is less marked, although at higher injection the trend of the curves suggests that the results from PL will result in derived currents *below* those from EL.

4.3 6J solar cell

For the 6J solar cell we used the same two excitation wavelengths, 532 nm and 730 nm, to excite luminescence in the top (AlGaInP and GaInP) and the middle (AlGaInAs and GaInAs) two subcells, respectively (Fig. 4b). The strong overlap in QE between the cells shown in Fig. 4a, made it very difficult to excite just one subcell. This might represent a problem at very high injection levels when luminescent coupling between subcells becomes a significant fraction of the total injected current [5].

Unfortunately, emission from the bottom subcells (GaInNAs and Ge) could not be measured, probably due to a combination of reduced luminescent yield and low sensitivity of our setup in this spectral region. As a consequence, the total IV curve could not be compared to the dark IV to support the validity of the model.

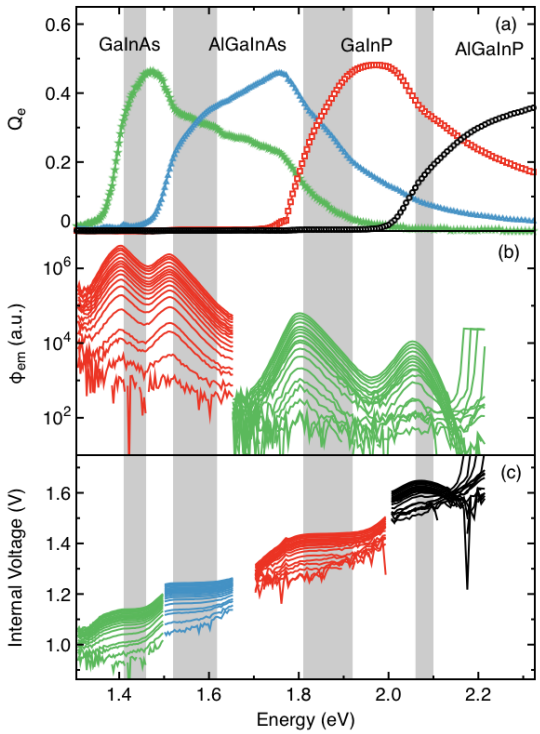

Figure 4: (a) External QE of the top and middle subcells of the 6J device. (b) PL emission when excited with the two lasers as a function of power. (c) Calculated internal voltages for each cell. The vertical colour bands indicate the regions that are averaged in each case to calculate the voltages and their uncertainties.

Fig. 5 shows the EL- and PL-derived IV curves. They follow the same trend already discussed in the 1J and 2J solar cells, with the PL-derived IV lying above the EL-based one. However, here it becomes clearer that both curves tend to the same values at higher injection.

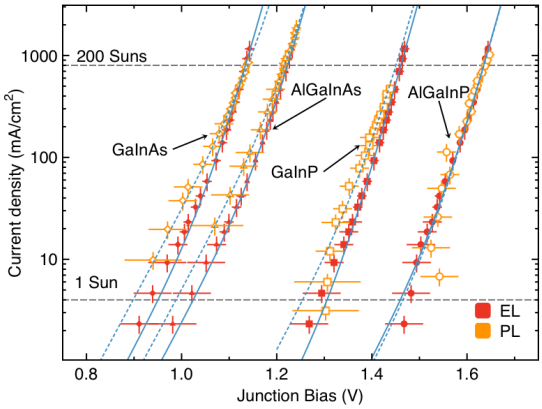

Figure 5: Implied IV curves from EL and PL for the top and middle junctions of the 6J solar cell. Blue lines indicate fits to a 2-diode model in each case.

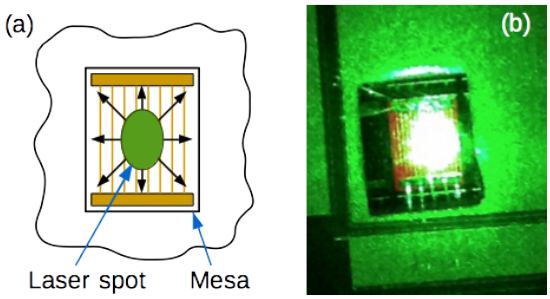

Figure 6: (a) Carriers photogenerated in the region of the laser spot travel in the plane of the sample and recombine in the whole mesa. (b) Picture of one of the devices, showing the bright green spot of the laser in the middle and red PL coming from the regions around.

5 DISCUSSION

5.1 The role of in-plane transport

Despite the agreement of voltages in all cases, it is clear that there is a discrepancy in estimating the current density when using El and PL, specially at low injection levels. Such discrepancy was already noted in Section 2 where we introduced Eq. 3: not all photogenerated carriers recombine in the region where they are generated; a significant fraction are transported laterally, further if the material has high conductivity, until they reach the end of the mesa (Fig. 6a). As a consequence, although generation takes place in the excitation oval described before, recombination takes place througout the device. This can be clearly seen in Fig. 6b where the bright, green spot of the laser in the centre of the sample is surrounded by red PL emission from the GaInP subcell coming out from the whole device.

To prove this point, we carried out a simple calculation, modelling the in-plane transport with a 1D-mesh of resistances and the solar cells as diodes. This model is used often with several degrees of sophistication

to estimate the dark currents and sheet resistance of silicon [6] and MJ [7] solar cells using EL or PL imaging. Fig. 7a shows a schematic representation of the model. Light is optically injected in the central nodes of the 1D circuit. Ideally, that photogenerated current should flow through the diodes of those nodes but in practice, some of it will flow away, towards the nodes in the dark.

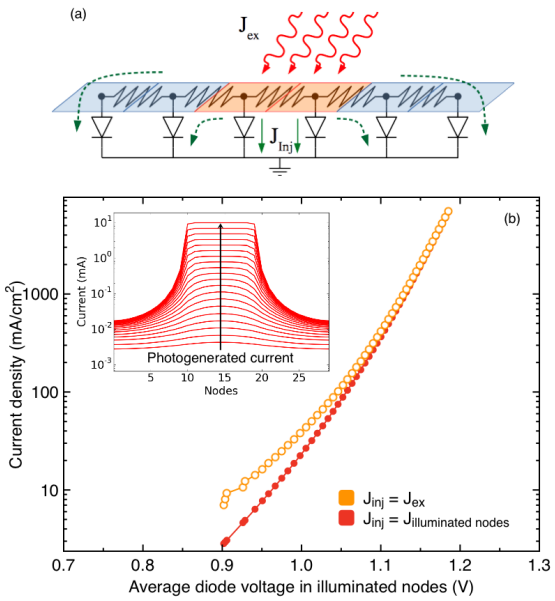

Figure 7: (a) Schematic representation of the 1D model for in-plane transport. Orange region represent the illuminated nodes. (b) Simulated IV curves for the two assumptions about the injection current. The inset shows the current flowing across each diode as a function of the photogenerated current.

Fig. 7b shows the resulting IV curves using the saturation currents obtained for the 1J GaAs in Fig. 2c and some sensible, but arbitrary, value for the resistors. At low injection, a large fraction of the photogenerated current will flow to adjacent nodes, therefore reducing the amount that is actually injected in the illuminated nodes (Fig. 7b, inset). As the injection increases, more current will flow to the adjacent nodes, increasing the voltage drop across the resistors and biasing the diodes of the illuminated region, making them more conductive. Overall, the current flowing away represent a smaller fraction that the photogenerated one, making the two IV curves to get closer. Ultimately, as the injection increases further, virtually all photogenerated current will flow through the illuminated nodes.

High in-plane conductivity of the material – meaning low resistance in the model – will lead to a larger discrepancy between both curves. The upper limit is found when photogenerated carriers are distributed homogeneously over the whole mesa. In this situation, the ratio between both IV curves is equal to the ratio between the area of the mesa and the area of the excitation spot. That is the case for the 1J solar cell (Fig. 2c) where the EL- and PL-based curves differ by a factor of 4 at all voltages, identical to the ratio of the areas. Conversely, lower conductivity will reduce the in-plane transport and therefore the EL- and PL-based curves will be similar, at least at higher injection. This is the general trend observed in all other cases.

It should be noted that this argument can be applied also to the EL: a low conductivity will mean that the injected region does not occupy the whole mesa, as we have assumed, but a smaller area, and therefore, we will be overestimating the current injected in the collection region. That could be the case for the GaInP subcell in the 2J solar cell. This situation can be observed in solar cells with high sheet resistance [7].

This comparison between the EL- and PL-based IV curves, together with a more elaborate model than the one of Fig. 7a (see for example Ref [7]), could allow for a very fast characterisation of the in-plane conductivities of the materials on standard, fully processed solar cells, giving information about their quality, their performance under inhomogeneous illumination conditions or the quality of the design of the metal grid.

As a stand-alone characterisation technique, however, it will be necessary to minimise the in-plane transport of photogenerated carriers in order to have a reliable PL-based IV curve. This means that the excitation spot must cover the whole sample – the mesa, in the case of devices – a situation where homogeneous illumination, or even sufficient injected current in the case of very large areas, might difficult to achieve, in silicon-based solar cells or in MJ solar cells for space.

It should be noted that the method does not involve taking images of the sample, such as in [7] or [8] and therefore it is expected to be much faster, more sensitive, computationally less intensive and cheaper, therefore more suitable for a manufacturing environment.

5.2 Speed and accuracy

All the results presented in Fig. 2, 3 and 5 support the claim that internal voltages of a MJ solar cell can be accurately estimated using a contactless and fast characterisation tool, as it is PL. In our case, each point in the IV curves takes from 10 to 100 ms to be measured, meaning that with a correct automation and exciting simultaneously with all lasers, the complete IV of all subcells in a MJ solar cell could be measured in a matter of 1-2 s, depending on the desired resolution.

Once the implied IV curves are known, solar cell parameters such as the saturation currents associated to n=1 and n=2 ideality factors or the V_{oc} and the FF at any injection level could be estimated for each subcell. For example, in the case of the 6J solar cell, at 200 Suns (see Fig. 5), the Voc would be: 1.14V, 1.22V, 1.46V and 1.64V for the GaInAs, AlGaInAs, GaInP and AlGaInP subcells, respectively.

For the voltages, the accuracy of the method depends on the accuracy of the measured Q_e, the luminescence and the temperature, as well as the calibration factor. While a 10% relative error in the Q_e or the luminescence only produces an absolute change in the voltage of around 2.6 mV each at room temperature, according to Eq. 2, the noise in the signal, the influence of the background, the tail of the laser and temperature drift with power increases that uncertainty, specially for low luminescence intensities. In the end, the latter is the main limitation of the method, shared with the EL-based IV curves: the solar cells have to emit enough light to be measured, meaning that poor quality materials or low injection conditions can not be measured with low sensitivity setups.

For the current, the main limitation is the good knowledge of the actual injected area. Assuming that lateral transport is negligible, then the uncertainty of the

injected current will be proportional to the uncertainty in the power of the laser and the uncertainty of the quantum efficiency at the wavelength of the laser, typically on the order of 3-5% for the latter.

6 CONCLUSIONS

In this work we have presented a PL-based IV characterization method for MJ solar cells that allows for a fast, contactless measurement applicable even in unfinished devices. Results have been presented for 1J, 2J and 6J devices. At higher injection conditions, the PL-based IV curves overlap to those obtained from EL measurements and normal dark IV measurements. At low injection, however, currents are overestimated in the PL experiments. We attribute this to in-plane carrier transport from the region under illumination to the region in the dark. This issue can be solved by using a larger illumination area, so the results support the validity of the technique as a characterization tool able of fast screening the internal IV curves of an arbitrary number of subcells in a MJ device.

7 ACKNOWLEDGEMENTS

We acknowledge the financial support from the EMRP Researcher Grant Contract NO. ENG51-REG3. EMRP is jointly funded by the EMRP participating countries within EURAMET and the European Union.

8 REFERENCES

[1] T. Trupke, R. a. Bardos, M. D. Abbott, and J. E. Cotter, *Appl. Phys. Lett.*, vol. 87, no. 2005, pp. 2013–2016, 2005.

[2] L. Lombez, M. Paire, A. Delamarre, G. El-hajje, D. Ory, D. Lincot, and F. Guillemoles, *2014 IEEE 40th Photovoltaic Specialist Conference (PVSC)*, 2014, 1–3.

[3] T. Kirchartz, U. Rau, M. Hermle, A. W. Bett, A. Helbig, and J. H. Werner, Appl. Phys. Lett., vol. 92, 123502, 2008.

[4] S. Philipps, W. Guter, E. Welser, J. Schöne, M. Steiner, F. Dimroth, and A. Bett, Chapter 1 in Next Generation of Photovoltaics SE - 1, vol. 165, A. B. Cristóbal López, A. Martí Vega, and A. Luque López, Eds. Springer Berlin Heidelberg, 2012, pp. 1–21.

[5] H. Nesswetter, N. R. Jost, P. Lugli, a. W. Bett, and C. G. Zimmermann, Appl. Phys. Lett., vol. 106, no. 2, p. 023903, 2015.

[6] H. Hoffler, O. Breitenstein, and J. Haunschild, *IEEE J. Photovoltaics*, vol. 5, no. 2, pp. 613–618, Mar. 2015, and references therein.

[7] H. Nesswetter, P. Lugli, A. W. Bett, and C. G. Zimmermann, IEEE J. Photovoltaics, vol. 3, no. 1, pp. 353–358, 2013.

[8] A. Delamarre, L. Lombez, and J. F. Guillemoles, *Appl. Phys. Lett.*, vol. 100, no. 2012, pp. 17–20, 2012.